frontiers in Marine Science

ORIGINAL RESEARCH
published: 18 September 2020
doi: 10.3389/fmars.2020.572166

Deep-Sea Habitats and Megafauna on the Slopes of the São Paulo Ridge, SW Atlantic

Jose Angel A. Perez[1], Lucas Gavazzoni[1], Luis Henrique P. de Souza[1], Paulo Y. Gomes Sumida[2] and Hiroshi Kitazato[3]*

[1] Laboratório de Estudos Marinhos Aplicados (LEMA), Escola do Mar, Ciência e Tecnologia (EMCT), Universidade do Vale do Itajaí (UNIVALI), Itajaí, Brazil, [2] Instituto Oceanográfico, Universidade do Estado do Pará, São Paulo, Brazil, [3] School of Marine Resources and Environment, Tokyo University of Marine Science and Technology, Tokyo, Japan

The São Paulo Ridge (SPR) is a 350 km-long linear geological feature located in the Continental Margin off Brazil (Latitude 28–29°S, Longitude 40–45°W). In 2013, the region was mapped during the SW Atlantic "Iata-Piuná" expedition and explored by a series of deep-sea dives of the manned submersible Shinkai 6500. A digital bathymetric model analyzed for seafloor morphology, delimited four major bathymetric sectors namely plateau, ridge crest, ridge escarpment and ridge foot. These sectors further enclosed 12 morphological features at smaller spatial scales (structural classes) including plains, valleys, peaks, terraces, and troughs. Video profiles across the depth gradient (4,219–2,644 m depths) revealed that the slopes of the SPR southern flank were gentle and terraced, mostly covered by biogenic sediments and interrupted by rocky cliffs/crests, dispersed outcrops and loose particles. The North Atlantic Deep Water (NADW) and Antarctic Bottom Water (AABW) overlaid at the escarpment along which they established colder (0.4–1.0°C; 4,200–3,400 m) and warmer (2.0–3.0°C; 3,400–2,600 m) habitats, respectively. Physical components were used to define seven seascape units in the ridge foot (2), escarpment (3), and plateau-ridge crest (2), where a total of 914 organisms of the epibenthic and benthopelagic megafauna were recorded. Over 70% of these records were sessile suspension feeders, including sponges (61.5%) and anthozoans (11.4%). Most taxonomic groups concentrated above 3,800 m, under the influence of NADW, where densities reached maximum values (mean 0.26 organisms.m^{-2}; 0.024–0.027 organisms.m^2 95% CI). Also, nearly half of megafauna records concentrated in patches delimited by the 3,800–3,300 m and 2,900–2,700 m isobaths. The deepest patch (3800–3300 m) coincided with the interface zone between AABW and NADW, where mixing processes create a density gradient. Evidences suggested that topography-related deep-water flow dynamics, and not substrate availability, drives benthic megafauna distribution at meso-habitat scale.

Keywords: São Paulo Ridge, Southwest Atlantic, depth gradients, NADW, AABW

OPEN ACCESS

Edited by:
Cristina Gambi, Marche Polytechnic University, Italy

Reviewed by:
Franziska Althaus, Commonwealth Scientific and Industrial Research Organisation (CSIRO), Australia
Alan Williams, Oceans and Atmosphere (CSIRO), Australia

****Correspondence:***
Jose Angel A. Perez
angel.perez@univali.br

Specialty section:
This article was submitted to Deep-Sea Environments and Ecology, a section of the journal Frontiers in Marine Science

Received: *12 June 2020*
Accepted: *24 August 2020*
Published: *18 September 2020*

Citation:
Perez JAA, Gavazzoni L, de Souza LHP, Sumida PYG and Kitazato H (2020) Deep-Sea Habitats and Megafauna on the Slopes of the São Paulo Ridge, SW Atlantic. Front. Mar. Sci. 7:572166. doi: 10.3389/fmars.2020.572166

INTRODUCTION

In recent decades, marine sciences, industry and conservation initiatives have turned their attention toward the Southwest Atlantic. The region has a critical role in the Atlantic Meridian Overturning Circulation (AMOC), whose dynamics influence poleward heat flux and global climate (Garzoli and Matano, 2011; Frajka-Williams et al., 2019). Deep components of AMOC are strongly affected by distinctive seafloor topographies, whose origin and morphology derive from geological events established throughout the history of South Atlantic Ocean expansion (Bassetto et al., 2000; Ussami et al., 2012). In association with topographic features, valuable mineral deposits have been mapped and explored (Hein et al., 2013) and deep ecosystems and biodiversity have been increasingly described (e.g., Perez et al., 2012; Kitazato et al., 2017; Jovane et al., 2019).

Particularly relevant in this context is the east-west trending system of topographic features that include the Rio Grande Rise, Vema Channel, São Paulo Ridge and São Paulo Plateau (**Figure 1**). With depths spanning 600–5,000 m, these rises and troughs interpose and provide channels for the flow of the deepest water masses of the Atlantic Ocean: the North Atlantic Deep Water (NADW) and the Antarctic Bottom Water (AABW). The former flows southwards along the West Atlantic, compensating the northward circulation of surface, central and intermediate waters, and maintaining mass balance in the Atlantic (Garzoli and Matano, 2011; Frajka-Williams et al., 2019). Transported by the Deep Western Boundary Current between 1,500 and 3,000 m depths, NADW circulation is constrained westward by the topography of Brazil's continental slope and transversely oriented seamounts and ridges, most notably the Vitoria-Trindade Chain, Rio Grande Rise and São Paulo Ridge (Stramma and England, 1999; McDonagh et al., 2002). Below 3,000 m, the AABW flows northwards, along the Southwest Atlantic basin and into the North Atlantic, often via abyssal conduits, most notably the 5,000 m-deep Vema Channel (McDonagh et al., 2002; Morozov et al., 2010). These deep-water masses, with their distinctive physical and chemical properties, interact with the seafloor contributing to the establishment of variable sedimentation regimes, habitats and biological communities. Descriptions of these relationships in the region are generally scarce but have progressively increased often driven by initiatives addressing the needs for conservation and future sustainable mineral exploitation (e.g., Sumida et al., 2016; Hajdu et al., 2017; Perez et al., 2018; Montserrat et al., 2019).

Bathyal communities tend to change continuously along depth gradients essentially because of depth-correlated conditions such as pressure, temperature and dissolved oxygen (Carney, 2005). Drastic changes, however, may be driven by spatial discontinuities in physical and chemical conditions, food supply, sedimentary regime, bottom currents, and major topographic features (Rex and Etter, 2010). These effects may be conspicuous in the São Paulo Ridge (SPR) whose southern flank forms a steep 2,200 m depth gradient that extends transversely to the predominant flow of the SW Atlantic deep circulation (Alberoni et al., 2019). The region was subject to geological studies in the 1970s and 1980s (e.g., Gamboa and Kumar, 1977; Gamboa and Rabinowitz, 1981) but remained mostly unexplored in terms of habitat configuration and biodiversity. In 2013 the SPR was targeted by a global expedition "Quelle 2013 – Quest for the limits of life" led by the Japan Agency for Marine-Earth Science and Technology (JAMSTEC), which searched for extreme deep-sea environments with the RV Yokosuka and the manned submersible Shinkai 6500 (Kitazato et al., 2017)[1]. An important finding of this exploration in the SPR was a deep whale fall with a well-established chemosynthetic community (Sumida et al., 2016; Cavalett et al., 2017; Shimabukuro et al., 2017; Shimabukuro and Sumida, 2019). In addition, the geological setting of the explored areas and a report of a fossil whale skull was provided by Ichisima et al. (2017). In this study we describe non-chemosynthetic benthic meso- and macro-habitats (*sensu* Greene et al., 2007) and megafauna along the SPR depth gradient and explore the effect of associated abiotic factors, including substrate, seafloor morphology and deep-water mass stratification. We further estimate large-scale distribution of benthic habitats in the SPR by analyzing bathymetry-derived terrain variables and classification of seafloor features. Benthic megafauna variability across different spatial scales will be discussed as a baseline and hypotheses for more detailed ecological studies in the future.

MATERIALS AND METHODS

Study Area

The São Paulo Ridge (SPR) is a 350 km-long linear geological feature located in the Continental Margin off Brazil, between 28–29°S and 40–45°W (**Figure 1A**). It is a component of the east-west trending Rio Grande Fracture Zone alignment that delineates the southern boundary of the São Paulo Plateau (Bassetto et al., 2000). As other aseismic ridges, the SPR is asymmetric with (a) a flat 2,000 m-deep northern flank, buried by sediments of the São Paulo Plateau, and (b) a steep southern flank (known as the São Paulo Escarpment), diving from 2,500 m-deep crests to a 4,200 m-deep foot (Gamboa and Rabinowitz, 1981; Alberoni et al., 2019). It is believed that SPR current morphology is largely derived from irregular submarine vulcanism that started in the Aptian period (∼120 m.a.), during the early South Atlantic Ocean expansion, when the SPR acted as a barrier obstructing the marine circulation toward the north and promoted the formation of a shallow environment where the deposition of a thick layer of evaporites resulted in the formation of the São Paulo Plateau (Gamboa and Rabinowitz, 1981; Bassetto et al., 2000; Ichisima et al., 2017). The southern flank interposes the northern flow of the Antarctic Bottom Water (AABW) generating countercurrents and eddies that mobilize sediments and form a trough delineating the deep contour of the ridge, also known as the São Paulo Channel (**Figure 1B**; Gamboa and Kumar, 1977; Alberoni et al., 2019). The NADW flows southward over the São Paulo Plateau, across the SPR crests and down over the escarpment where it overlays the AABW.

[1]https://www.jamstec.go.jp/quelle2013/e/

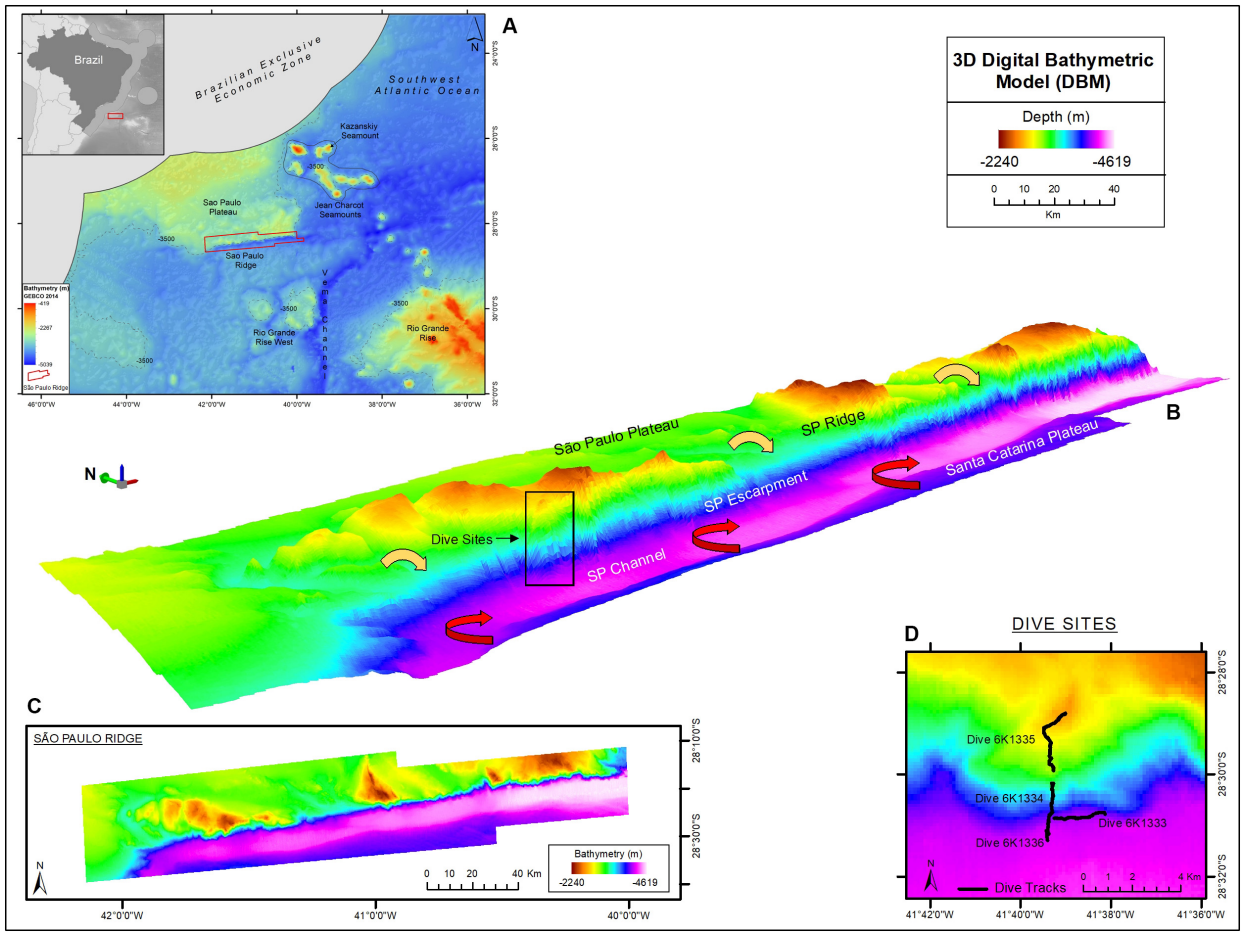

FIGURE 1 | The São Paulo Ridge (SPR) outlined in the SW Atlantic seafloor map **(A)**, 3D **(B)** and 2D **(C)** representations of the Digital Bathymetry Model. The box in the 3D bathymetry map indicates the area of deep-sea dives whose tracks are represented in detail in **(D)**. Circulation patterns of the North Atlantic Deep Water and Antarctic Bottom Water are represented by the yellow and red arrows, respectively. Projection World Mercator/WGS 84. Datum UTM 25 South.

Analyzed Data

Data on SPR seafloor benthic habitats and megafauna were acquired during a research cruise conducted by the RV "Yokosuka" in 2013, under the "Iata – Piuná" consortium established between the Japan Agency for Marine-Earth Science and Technology (JAMSTEC), the Oceanographic Institute of University of São Paulo (IOUSP) and the Geological Survey of Brazil (CPRM) (Kitazato et al., 2017). The SPR area was explored between April 23 and 27 and included swath bathymetry and deep-sea dives of the manned submersible Shinkai 6500.

Bathymetric data were acquired during along-ridge transects with a 12 kHz hull-mounted Multibeam Echosounder System (MBES), integrated Differential Global Positioning System (DGPS) and compensated by the Inertial Measurements System (IMU). The data were filtered to remove spurious depth records and submitted to methods of linear interpolation to produce a Digital Bathymetric Model (DBM) with a cell size of 123 m. Video transects were produced during four deep-sea dives along a complete SPR southern flank depth profile, from 4,219 to 2,644 m depths (**Figure 1** and **Table 1**). Dives 6K1333 and 6K1336 explored the abyssal region at the foot of the ridge. Part of these dives were dedicated at the study of a whale-fall carcass environment, encountered at 4,204 m depth, previously described by Sumida et al. (2016) and excluded from this study. Dives 6K1334 and 6K1335 described the seafloor along the depth gradient of the São Paulo Escarpment. All dives involved approximately 4 h of activities near the seafloor, including photo/video recording, geological and biological sampling. Video data was acquired by two HD-TV color video cameras, both positioned at the bow, 1.7 m above the vehicle's bottom (Nakajima et al., 2014). Camera 1 angled obliquely 40° toward the seafloor and recorded continuously a fixed area ahead the bow of the submersible (horizontal acceptance = 90°, vertical acceptance = 57°). Camera 2 was mobile (pan – tilt) and was used for detailed observations of habitat features and megafauna species. Continuous information of date/time, depth (and altitude in meters) and the vehicle's heading (in degrees) were overlaid in the videos. Horizontal position (latitude, longitude) was estimated by SSBL (Super Short Base Line) method which required a transponder mounted on the submersible and an

TABLE 1 | Summary of deep-sea dives conducted by the manned submersible Shinkai 6500 on the São Paulo Ridge, SW Atlantic.

Dive	Date	Latitude	Longitude	Depth (m)	Duration (h)
6K1333	23 April 2013	28°30′52″S	41°39′15″W	4,088–3,993	4.2
6K1334	24 April 2013	28°31′09″S	41°39′23″W	4,208–3,297	4.4
6K1335	25 April 2013	28°29′55″S	41°39′16″W	3,060–2,644	4.9
6K1336	26 April 2013	28°31′19″S	41°39′24″W	4,219–4,193	4.5

array of transducers on the hull of the RV Yokosuka. In this method the position is estimated by (a) phase lag measured from angles of received sound waves, and (b) distance calculated from their traveling period. Records of latitude and longitude were transformed into easting and northing (UTM) to estimate the linear distance covered by the submersible. The area covered by video transects was calculated by multiplying this linear distance by the mean lower width (MLW) of images taken every 6 s, following the equation proposed by Jones et al. (2009) for oblique videos with cameras facing the imaging path:

$$MLW = 2\sin(0.5\theta)\sqrt{\alpha\sin(90-\delta-0.5\omega)^2+\alpha^2}$$

where α is the altitude of the camera, θ and ω are the camera's horizontal and vertical acceptance angles, respectively, and δ is the angle of the camera from vertical (Nakajima et al., 2014). Measurable uncertainty in area estimations derived from variability in α along video transects. Bootstrap 95% confidence intervals of MLW were calculated for video transects or segments of it, using the quantile method.

Megabenthos specimens were collected by the submersible's manipulators and slurp-gun, photographed on board and stored in ethanol (75%) and formalin for posterior identification by specialists in the National Museum (Federal University of Rio de Janeiro) where they were cataloged.

Videos, sample records and oceanographic data and metadata are available in "DARWIN – Data and Sample Research System for Whole Cruise Information in JAMSTEC[2]."

Seafloor Morphometric Analysis

The DBM was analyzed for seafloor morphology and segmentation (Brown et al., 2011). This process included the transformation of bathymetry data into secondary-derived layers (terrain variables) using the algorithm package Benthic Terrain Modeler (BTM) (Walbridge et al., 2018) contained in ArcGIS Desktop® 10.2.2. Variables with the greatest potential for the description of benthic habitats at the corresponding spatial scales were chosen, including surface gradients (slope, aspect), relative depth (Bathymetric Position Index – BPI) and surface rugosity (Vector Roughness Measurement – VRM) (Wilson et al., 2007; Walbridge et al., 2018). BPI is a neighborhood analysis function of the mean depth around each cell in the DBM. Positive values correspond to features and regions that are higher than the surrounding area which characterize ridges; negatives values would represent depressions on the seafloor. Values equal or near zero are either flat or constant slope area (Walbridge et al., 2018).

The procedures for seafloor segmentation (**Figure 2**) started with overlaying 23 bathymetric profiles on the DBM, transversal to the bathymetric gradient of the São Paulo Escarpment (**Supplementary Figure 1**) for visual interpretation. Along each profile, the variables BPI-broad (annulus = 300 pixels ∼ 36,900 m), BPI-fine (annulus = 60 pixels ∼ 7,380 m) and slope were extracted and analyzed individually in order to identify Zonal and Structural classes (*sensu* Erdey-Heydorn, 2008). Zonal classification described broad scale surficial characteristic of the seafloor. Classes representing the main bathymetric components were visually defined, and had their boundaries delimited by depth and values of BPI-broad and slope (i.e., averages across the 23 transversal bathymetric profiles). Within each Zonal class, surficial characteristics of the seafloor were then described to a greater detail (Structural classification) using terrain variables BPI-fine and slope. Structural classes were again visually defined and delimited by maximum and minimum values of depth, BPI-fine and slope values (i.e., averages across the 23 bathymetric profiles). A classification table was then built, summarizing lower and upper limits of depth, slope, BPI-broad and BPI-fine for all visually defined Zonal and Structural classes (**Supplementary Table 1**). The classification table was then used as input data for semi-automated classification of new adjusted classes by BTM's Classify Benthic Terrain tool. Such classification procedure (followed by spatial representation of the resulting classes) was performed several times until the spatial segmentation was considered satisfactory (**Figure 2**). Each model run was conducted after manual adjustments of the terrain variable values delimiting structural classes, and/or the creation of new intermediate classes.

Seascape Classification

Each video produced by camera 1 was initially observed to record changes in depth, altitude, submersible activities and image visibility. Also, seafloor features relevant for habitat classification (following Greene et al., 1999) were selected, namely: substrate texture, particle sizes, relief and others. These features were organized in a scale of "substrate types," represented by capital letters, where: R = rocky ridge with rugged surface; F = flat rocky pavement with plain or granulated surface; B = loose boulders (>25.5 cm); C = cobbles (>6.5 cm and <25.5 cm); P = pebbles (>2 cm and <6.5 cm); G = gravel (>4 mm and <2 cm); U = unconsolidated substrate varying from fine mud to coarse sand.

A second analysis of these videos included only segments when the submersible was moving ahead. During these segments, substrate types were attributed to 1-min video intervals using a two capital letters system; the first referring to the substrate type covering more than 50% of the visible seafloor, and the second to the substrate covering between 30 and 50%. For example, a segment where seafloor was mostly unconsolidated (e.g., covered by biogenic sediment) with variable amounts of scattered pebbles was codded as UP. Also, when only one type of substrate was visible during the observed interval the correspondent letter was duplicated (e.g., UU = seafloor completely covered by

[2]http://www.godac.jamstec.go.jp/darwin/

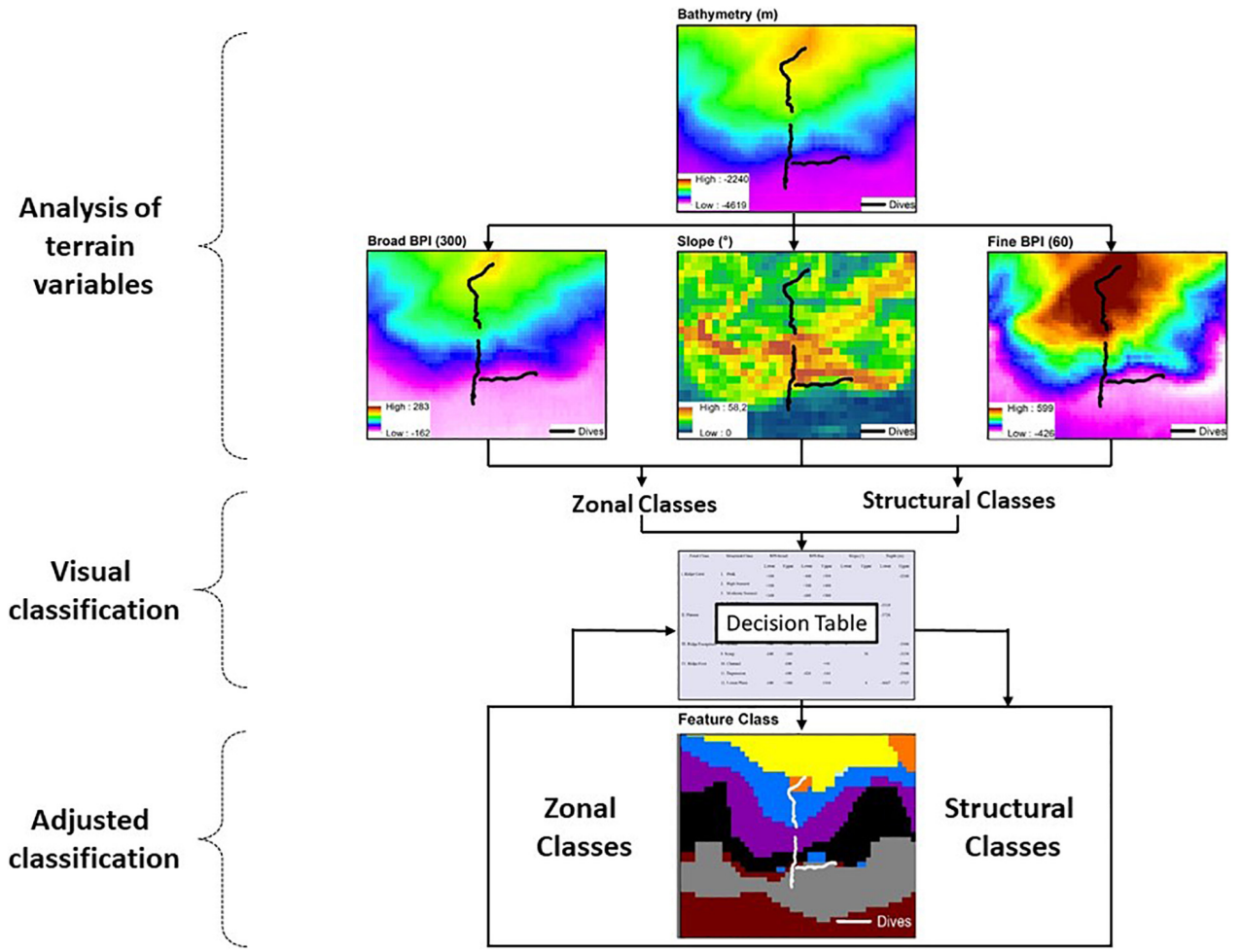

FIGURE 2 | Flow diagram describing the seafloor classification procedure applied to the São Paulo Ridge multibeam bathymetry including the analysis of depth and depth-derived terrain variables, visual classification and construction of a classification table and adjusted classification using the Benthic Terrain Modeler (BTM) (Walbridge et al., 2018).

sediments). These combinations of two substrate types were defined as "bottom types" (Greene et al., 2007; Tissot et al., 2007; Tissot, 2008).

Seascapes units were mainly defined by one or more dominant bottom types regularly combined along a continuous segment of the seafloor. Adjacent seascapes were delimited by an abrupt change in the dominant bottom type (or bottom type combination) observed for more than 10 s along the video track, indicating the end of a seascape unit and the beginning of a new one. Bottom types that contrasted with the dominant ones but did not persist long enough along the video track (e.g., a patch), were not considered a new seascape unit, but as part of the current seascape substrate variability. Descriptions of seascape units were complemented by "modifying" elements (e.g., currents, bioturbation), relief and slope (Greene et al., 1999), as well as by the influence of AABW and NADW on the seafloor. This influence was estimated by temperature and salinity data recorded continuously during the dive track by the submersible's CTD. Mixing percentages of these water masses during the dives were calculated according to Mamayev (1975).

Megafauna Diversity

Videos produced by cameras 1 and 2 were analyzed for visible megafauna. Life forms smaller than approximately 5 cm and/or visible in images taken above 2-m altitude were not included in the analysis. Otherwise, videos were stopped at each sighting and recorded the organism type ("morphotype") along with associated information, including date, time, depth (m), altitude (m), and heading (in degrees). Morphotypes were classified in higher taxa (Phylum, Class, Orders) and their consistency was double checked by repeating the analyses of videos produced by both camera 1 and 2. When no morphotypes could be confidently assigned to a given observed organism after these repeated analyses, it accounted for higher taxa quantification only. Some morphotype identifications to family, genus and species level were possible through collaboration with deep-sea fish and invertebrate taxonomists, and with the aid of deep-sea

fauna image databases (e.g., OER's Benthic Deepwater Animal Identification Guide[3] and others).

Megafauna spatial distribution and abundance was analyzed by representing density of total recorded megafauna and/or taxonomic groups as a function of the depth strata and seascape units. Density was calculated by dividing organism numbers by the mean estimated areas covered by video transects (expressed as individuals. m^{-2}), and their 95%CI limits.

RESULTS

Seafloor Segmentation

The SPR is depicted as the southern margin of the São Paulo Plateau, which extends to the north as 3,000 m-deep plane areas (**Figure 1**). Along the border of the plateau, prominent ridge crests rise to 2,200 m depths, over 1,000 m above the plateau level. These crests are separated by plane areas and channels that extend to the edge of the plateau, possibly characterizing paths of deep-water flow. The margin of the plateau is continuously bordered by the São Paulo Escarpment that forms a south – southeast facing wall, which is (a) higher/steeper in sectors adjacent to the plateau crests (**Supplementary Figure 2**, e.g., profiles 3, 11, and 19) and (b) lower/gentler in sectors adjacent to plane areas in between the ridge crests (**Supplementary Figure 1**, e.g., profiles 8, 15, and 22). The deep edge of the escarpment is connected to the 4,100–4,300 m-deep São Paulo Channel, a trough extending continuously along the SPR. To the south of this channel, the seafloor rises into a 4,000 m-deep plain area that is part of the Santa Catarina Plateau (**Figure 1**).

The spatial representation of BPI-broad delineated the areas comprised by broad bathymetric components, including the São Paulo Plateau, plateau crests, São Paulo Escarpment, São Paulo Channel and Santa Catarina Plateau (**Figure 3**). Secondary seafloor structures were evidenced from the spatial analysis of BPI-fine and included valleys and channels on the São Paulo Plateau, as well as discontinuities of the São Paulo Channel. Slope, aspect (easterness and northerness) and roughness (VRM) provided refined spatial representations of (a) channels and valleys bordering the plateau crests, and crossing the margin of the São Paulo Plateau, and (b) the escarpment, depicted as a steep, southern-faced roughed terrain (**Figure 3**). These were seafloor topography subject to classification by the morphometric analysis (see below).

The seafloor classification procedure resulted in 12 Structural Classes (**Figure 4**) enclosed within four Zonal Classes. Descriptors (upper and lower limits of depth, terrain variables and slope) and names attributed to each on of them are presented in **Supplementary Table 1**. The plateau (Zonal Class II) comprises plains (Class II.5), valleys (Class II.6), and gentle slopes (Class II.7) which were shallower than 3,700 m and with less than 5° slope. The SPR crest (Class I) is composed of seamount-like summits of high (Class I.2), moderate (Class I.3), and low (Class I.4) altitudes, some of the former topped by 2,240 m-deep peaks (Class I.1). Bordering the edge of the plateau, the São Paulo Escarpment (Class III) is formed by an upper terrace (Class III.8) followed by a deeper scarp (Class III.9). At the ridge foot (Class IV), the São Paulo Channel (Class IV.10) runs continuously along the entire SPR extension, sometimes bordered by local depressions next to the escarpment (Class IV.11), and connected to the south to the deep plains of the Santa Catarina Plateau (Class IV.12) (**Figure 4**).

Seascapes

The deep-sea dives crossed four zonal classes: ridge foot, ridge escarpment, plateau and ridge crest (**Figure 4C**). Seafloor texture was dominated by biogenic sediments usually mixed with scattered rocky particles (UP, UC), outcrops and crests (UF, UR) (**Supplementary Table 2**). These bottom types were recorded for over 56% of the observation time, followed by bedrock outcrops (RU + RC = 33.5%). Areas entirely covered by rocky substrata (e.g., RC, RR, RP, FP, PC) were recorded in 7.1% of the observed time. Most of the area observed (>90%) corresponded to gentle slopes (5–30°). Steep slopes (>30°) occurred in 2% of the observed area and only in the ridge escarpment.

Texture classification, slope, water masses and modifying elements allowed the differentiation of seven seascape units (**Table 2**). The "Abyssal Mud Field" (AMF), was characterized by an undulated sediment surface covering the São Paulo Channel seafloor, with isolated patches of pebbles and bedrock outcrops (UP, UR). This seascape dominated images produced by dive 6K1333 that explored a linear track along the foot of the ridge, in eastward direction over the 4,000–4,100 m isobaths. The effect of AABW flux was noticeable in this seascape, usually producing regular sand waves (**Table 2**). Adjacent do AMF, the "Debris Field" (DF) extended along the deep border of the escarpment generally characterized by a mixture of cobbles, pebbles, and boulders, interspersed with biogenic sediments (UC and UP). These bottom types, recorded in 64.5% of the total observation time of this seascape (**Supplementary Table 2**), were often associated with landslide signs and coated by a thin sediment cover (**Figure 5A**).

Moving into the lower section of the ridge escarpment (above 4,100 m depths) the seascape was dominated by a steep and roughed bedrock surface, the "Bedrock Cliff" (BC) (**Table 2**). Rocky ridges sometimes covered by piles of loose cobbles (RU and RC) dominated the seafloor (64.5% of the observation time, **Supplementary Table 2**) (**Figure 5B**). Small amount of sediments accumulated in cracks and crevices, and thinly covered bedrock particles. This seascape unit was interrupted at approximately 4,070–3,998 m depths by a narrow terrace formation, the "Granular Flat" (GF) (**Table 2** and **Figure 5C**), where flat bedrock pavements were usually covered by pebbles and variable amounts of sediments (FP + FU = 71.4% of the observation time, **Supplementary Table 2**). A positive (convex) relief characterized the upper section of the escarpment (above 3,366 m depths), where the seascape "Bedrock Crest" (BCR) was defined by a mixed substrate formed by bedrock outcrops and sediment ponds (RU) (**Table 2** and **Figure 5D**). This seascape unit was also observed in the ridge crest, between 2,578 and 2,657 m depths (**Figure 5**).

[3]https://oceanexplorer.noaa.gov/okeanos/animal_guide/animal_guide.html

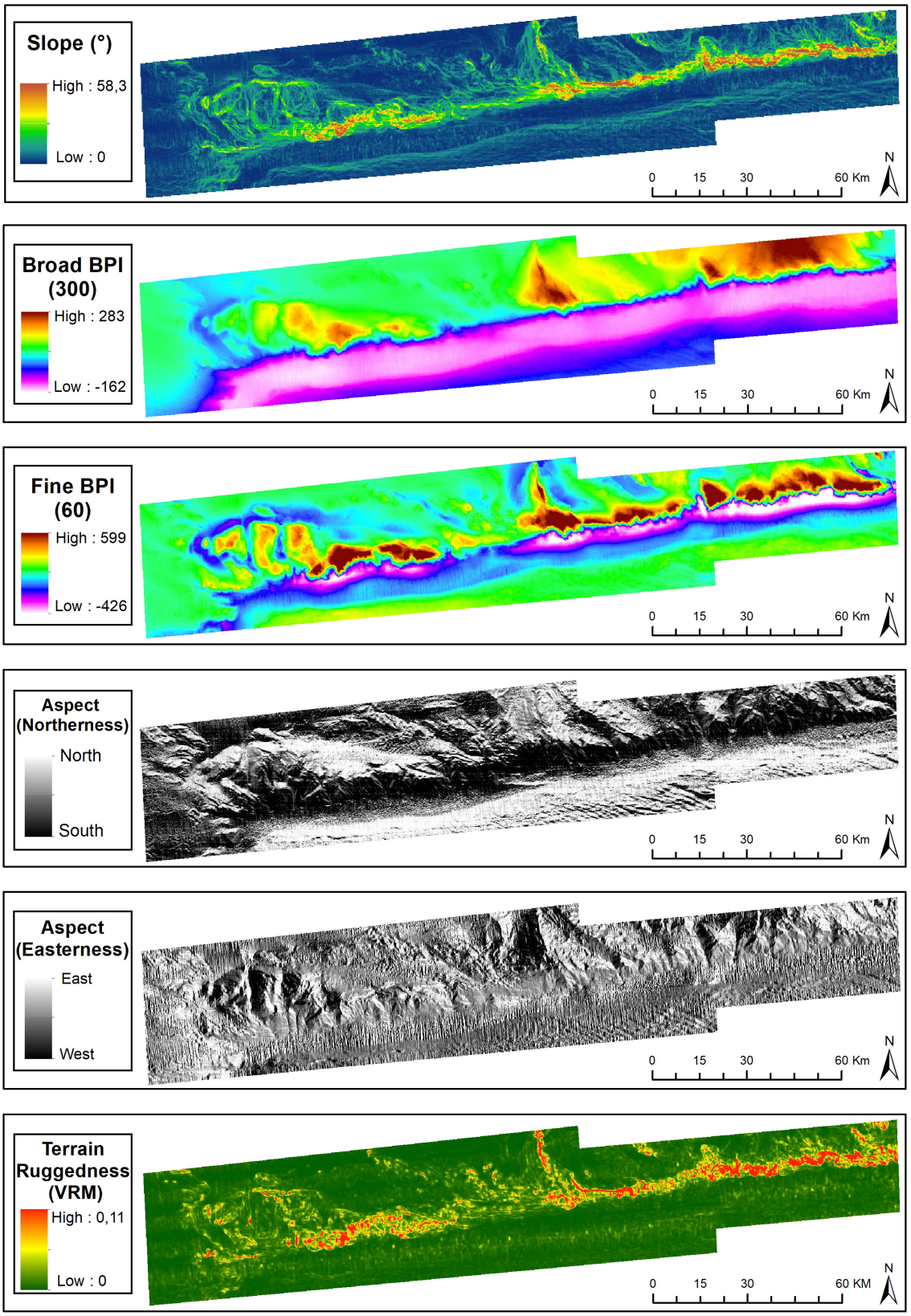

FIGURE 3 | Terrain variables derived from the digital bathymetric model of the São Paulo Ridge. Projection World Mercator/WGS 84. Datum UTM 25 South.

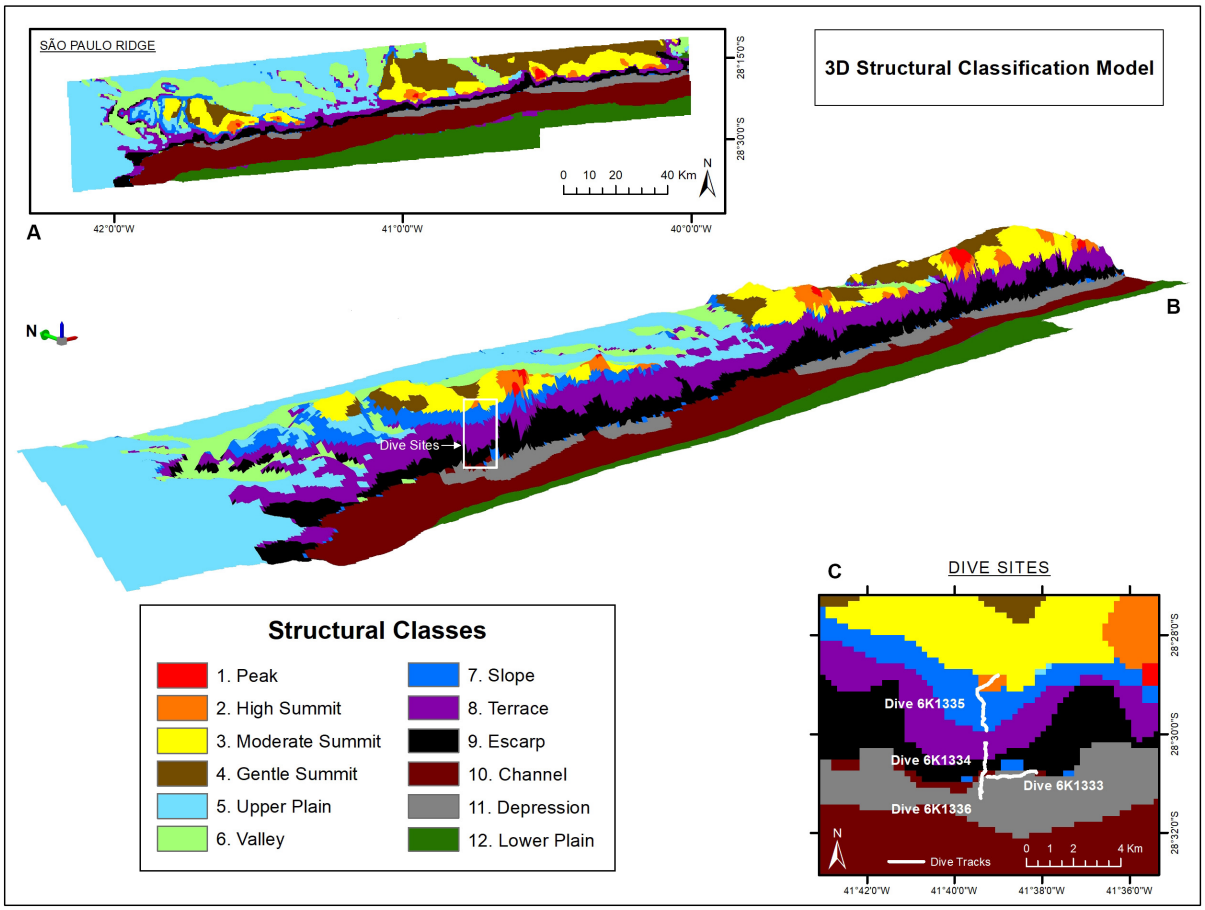

FIGURE 4 | São Paulo Ridge seafloor classification based on bathymetry and depth-derived terrain variables. **(A,B)** 2-D and 3-D spatial representation of Structural Classes (white box = dive area). **(C)** Detail of the dive exploration sites.

At the ridge plateau and the adjacent ridge crest, flat sedimented areas (UU), occasionally with sparse patches of pebbles and cobbles (UP, UC), formed a seascape unit called "Mud Terrain" (MT) (**Table 2**). Sediment surface was generally smooth, but often modified by animal tracks (**Figure 5E**). The ridge plateau also included a slightly convex "Granular Crest" (GCR) (**Table 2** and **Figure 5F**) covered by pebbles, cobbles and soft sediments (RU + UP = 82.2% of observation time **Supplementary Table 2**).

Temperature of the water mass overlaying the seafloor ranged between 0.45 and 3.11°C, and salinity between 34.59 and 34.94 psu (**Supplementary Figure 2**), well within the limits of the NADW and AABW (according with Morozov et al., 2010). The AABW-NADW interface, delimited by the isotherms 1.8–2.0°C (Zhao and Thrunherr, 2017) at 3,409–3,433 m depths in the ridge escarpment (**Supplementary Figure 3**), coincided with the boundary between seascapes BC and BCR (**Figure 5**). Density decreased sharply in this depth zone characterizing mixing processes, i.e., warming of AABW (Zhao and Thrunherr, 2017) (**Supplementary Figure 2**). AABW influence predominated on seascape units AMF, DF and GF (>82% mixing) and NADW influence predominated on seascapes BCR, MT, and GCR (>85% mixing) (**Table 5**). Mixing percentages of these water masses varied widely on BC (AABW 20–93%, NADW 7–80%). Highest temperatures (2.75–3.10°C) were recorded at the plateau – ridge crest (3082–2676 m) and lowest (0.4–0.6°C) at the ridge foot (4,208–4,014 m).

Megafauna

A total of 914 organisms of the epibenthic and benthopelagic megafauna were recorded during 700 min of SPR seafloor observation. Over 70% of the records were sessile suspension feeders, including sponges (62.8%) and anthozoans (11.6%). These were followed by shrimp-like crustaceans (11.3%) and fish (Actinopterygii, 8.7%) (**Table 3**). A list of identified taxa is presented in **Table 4**.

Megafauna records were usually sparse (<0.01 individuals.m^{-2}) along the SPR depth gradient, but two patches of moderate concentrations (0.07–0.30 individuals.m^{-2}) mostly of suspension feeders, occurred at 3,800–3,300 m, and 2,900–2,700 m depth intervals (**Figure 6**). The former patch occurred in the ridge escarpment and the BC and BCR seascapes. The latter patch occurred at the ridge crest and within the reach of the GCR, MT and BCR seascapes. Both depth zones were

TABLE 2 | Classification of seafloor explored during deep-sea dives in the São Paulo Ridge, SW Atlantic into seascape units according with Greene et al. (1999).

Seascape unit	Class (Meso-Macrohabitat)	Subclass (Macro – Microhabitat)	Modifications
Abyssal Mud field (AMF)	Undulated sediment floor	Slope: Sloping (mean slope = 11°) Texture: Mud (carbonate ooze). Buried debris (cobbles, pebbles, pavements) that outcrop in small patches. Temperature: 0.45–0.75°C Salinity: 34.64–34.72 psu Water mass: AABW	• Sand waves • Lebensspuren
Debris field (DF)	Submarine slump	Slope: Sloping (mean slope = 11°) Texture: Irregular piles of cobbles and boulders (landslides). Sediment (mud) ponds (Figure 6A) Temperature: 0.45–0.61°C Salinity: 34.69–34.77 psu Water mass: AABW	• Thin sediment cover (1–5 cm) • Sand waves and lebensspuren (on the surface of sediment ponds)
Bedrock cliff (BC)	Scarp, wall	Slope: Steeply sloping (mean slope = 30°) Texture: Rough bedrock surface (igneous). Loose cobbles and boulders (Figure 6B) Temperature 0.46–2.25°C Salinity: 34.59–34.87 psu Water mass: Mixed AABW and NADW	• Dusting sediment cover (<1 cm) • Small sediment packs accumulated in cracks and crevices • Suspension feeders (mostly sponges)
Granular flat (GF)	Narrow terrace	Slope: Sloping (mean slope = 15°) Texture: Granular surface formed by pebbles, cobbles and accumulated sediments (Figure 6C) Temperature: 0.50–0.66°C Salinity: 34.66–34.71 psu Water mass: AABW	• Dusting sediment cover (<1 cm)
Bedrock crest (BCR)	Slope crest (convex)	Slope: Steeply Sloping (mean slope = 30°) Texture: Mixed substrate – Rough bedrock (high relief ∼1–2 m). Sediment ponds (Figure 6D) Temperature: 2.24–3.06°C Salinity: 34.74–34.94 psu Water mass: NADW	• Dusting sediment cover (<1 cm) • Sand waves and lebensspuren (on the surface of sediment ponds) • Suspension feeders (sponges and cnidarians) on bedrock • Holothurians (on sediment ponds)
Mud terrace (MT)	Undulated sediment floor	Slope: Sloping (mean slope = 20°) Texture: Mud (carbonate ooze) (Figure 6E) Temperature: 2.60–3.12°C Salinity: 34.86–34.94 psu Water mass: NADW	• Sand waves • Lebensspuren
Granular crest (GCR)	Slope crest (convex)	Slope: Sloping (mean slope = 17°) Texture: Granular surface formed by pebbles, cobbles, and accumulated sediments (Figure 6F) Temperature: 2.82–2.98°C Salinity: 34.88–34.94 psu Water mass: NADW	• Dusting sediment cover (<1 cm)

covered by hard substrata (e.g., outcrops or loose particles), but also included a variable coverage of sediments.

Most taxonomic groups were observed above 2,900 m and were associated with mixed substratum in the BCR seascape (**Table 3**). Nearly 60% of all records of Porifera occurred in this seascape being largely represented by two species: a pedunculated sponge, Family Dendoricellidae (cf *Pyloderma* sp., Demospongiae), and *Poliopogon amadou* (Hexactinellida) (**Figure 7**). Corals (Anthipataria and Alcyonacea) also tended to occur deeper, between 3,300 and 3,800 m, on the ridge escarpment (Seascape BC). 74.3 and 74.0% of crustaceans and echinoderms, respectively, were recorded below 2,900 m (**Table 3**). The latter was dominated by Holothuroidea, Order Elasipodida, including *Psychropotes semperiana*, *Benthodites* sp., and *Enypniastes* sp. These were observed in BCR usually occurring on sediment ponds. Nearly 44% of fish records concentrated in the 2,700–2,900 m depth stratum (**Table 3**). One

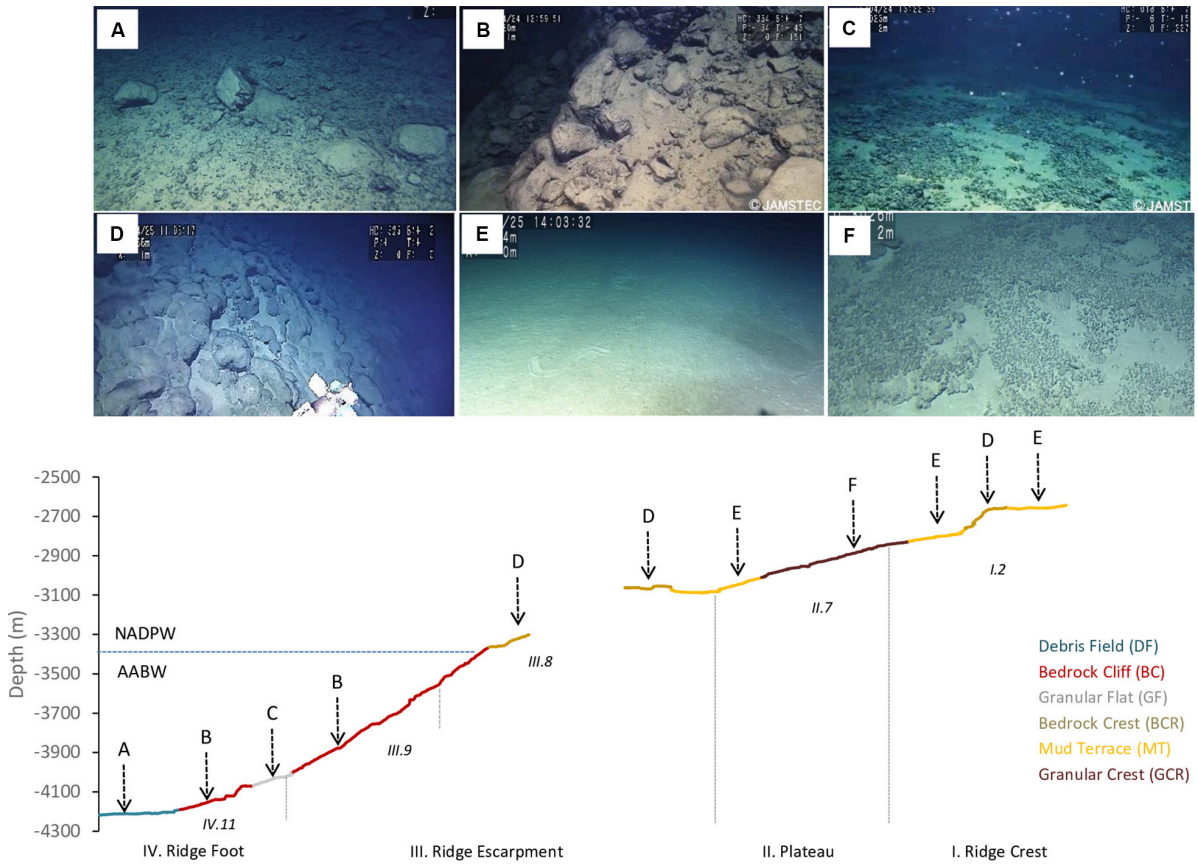

FIGURE 5 | Seascape units differentiated during deep-sea dives in the São Paulo Ridge, SW Atlantic, and their distribution along the depth profile. **(A)** Debris field (DF), **(B)** Bedrock cliff (BC), **(C)** Granular flat (GF), **(D)** Bedrock crest (BCR), **(E)** Mud terrace (MT), **(F)** Granular crest (GCR). Also indicated the Zonal and Structural classes defined based on the seafloor morphometric analysis. The blue line depicts the potential depth boundary between the AABW and NADP.

TABLE 3 | Summary of records of epibenthic and benthopelagic megafauna observed during exploratory deep-sea dives in the São Paulo Ridge, SW Atlantic.

	Cnidarians	Poriferans	Crustaceans	Fish	Echinoderms	Others	Total numbers
Seascape							
GCR	1.0	12.1	14.9	**43.6**	14.0	21.1	125
MT	8.7	15.8	26.7	19.2	22.0	21.1	151
BCR	**45.2**	**59.6**	21.8	7.7	**34.0**	**31.6**	427
GF	1.0	0.2	2.0	0.0	4.0	0.0	6
BC	**36.5**	10.1	13.9	12.8	8.0	0.0	123
DF	1.0	0.5	5.9	6.4	6.0	10.5	18
AMF	6.7	1.6	14.9	10.3	12.0	15.8	45
Depth strata							
<2,700 m	8.7	**41.6**	6.9	10.3	10.0	0.0	263
2,700–2,900 m	17.3	**34.0**	18.8	**43.6**	16.0	**47.4**	270
2,900–3,300 m	16.3	6.6	21.8	14.1	22.0	26.3	98
3,300–3,800 m	**47.1**	12.6	21.8	11.5	26.0	0.0	164
>3,800 m	10.6	5.2	**30.7**	20.5	26.0	26.3	45
Total*	11.6	**62.8**	11.3	8.7	5.6	2.1	
Total numbers	104	562	101	78	50	19	914

Numbers are column percentages of main taxonomic groups in seascape units and depth strata. Records in bold highlight important occurrences within each taxonomic group (>30%). The bottom (Total) line includes overall percentages of the taxonomic groups. Total numbers are total organism counts.*

TABLE 4 | Taxa identified during deep-sea dives in the São Paulo Ridge, SW Atlantic.

Phylum	Class	Order	Family	Species or tag name	Seascape
Porifera	Hexactinellida	Amphidiscosida	Pheronematidae	***Poliopogon amadou***	BCR
		Lyssacinosida	Euplectellidae	***Euplectella*** sp.	MT
	Demospongiae	Poecilosclerida	Dendoricellidae	cf. Pyloderma sp.	BCR
Cnidaria	Anthozoa	Antipatharia	Schizopathidae	*Bathypathes* sp.1	BC
				Bathypathes sp.2	DF
		Alcyonacea	Isididae	Keratoisidinae sp1.	BCR
				Keratoisidinae sp2	BC
			n.d.	Stolonifera sp.1	AMF
		Actiniaria	Actinoscyphiidae	Fly trap sp.1	AMF
Annelida	Polychaeta	Phyllodocida	Polynoidae	Scaled Worm sp.1	BCR
Arthropoda	Malacostraca	Decapoda	Munidopsidae	***Munidopsis*** sp.	DF
			Paguridae	Paguridae sp.1	BCR
		n.d.	n.d.	Shrimp-like sp.1	Various
		n.d.	n.d.	Shrimp-like sp.2	Various
Mollusca	Cephalopoda	Octopoda	Opisthoteuthidae	***Grimpoteuthis*** cf. ***discoveryi***	AMF
			Cirroteuthidae	***Cirrothauma murrayi***	BCR
Echinodermata	Holothuroidea	Elasipodida	Psychropotidae	***Psychropotes semperiana***	AMF
				Benthodytes sp.	BCR
			Pelagothuriidae	*Enypniastes* sp.	BC
	Asteroidea	Paxillosida	Astropectinidae	***Dytaster grandis nobilis***	MT
		Brisingida	Brisingidae	***Novodinia antillensis***	AMF
	Ophiuroidea	n.d.	n.d.	Ophiuroidea sp1.	DF
	Echinoidea	n.d.	n.d.	Echinoidea sp.1	AMF
Chordata	Actinopterygii	Aulopiformes	Bathysauridae	*Bathysaurus* sp.	DF
			Ipnopidae	*Bathypterois cf longipes*	BCR
				Bathypterois grallator	MT
		Gadiformes	Macrouridae	*Coryphaenoides armatus*	DF
				Macrouridae sp.1	BC
		Notacanthiformes	Halosauridae	*Aldrovandia* sp.	GCR
		Ophidiiformes	Ophidiidae	*Spectrunculus crassus*	DF
				Acanthonus armatus	GCR
				Bathyonus sp.	BC

Seascape units where the identified taxa occurred or were most frequent are indicated in the last column. Species in bold were identified from taxonomic analysis of collected organisms. n.d., not determined.

species, *Acanthonus armatus* (Ophidiiformes, Ophidiidae) was particularly abundant in association with the GCR seascape (**Figure 7D**).

Epibenthic and benthopelagic megafauna was recorded within a total area estimated in 35609.4 m^2 (34076.6–37236.8 m^2 95% CI). Mean density was 0.026 individuals.m^{-2} (0.024–0.027 individuals.m^2 95% CI) decreasing progressively with depth (0.130–0.005 individuals.m^{-2}, **Table 5**). The sectors above 3,300 m, including GCR, MT and, BCR seascapes, exhibited more elevated concentrations of megafauna, all of them under a prevailing influence of NADW (usually > 80%, **Table 5**). Upper sectors of BCR (<2,900 m) exhibited the highest fauna concentrations (0.328 individuals.m^{-2} – 0.300–0.360 95%CI) largely dominated by sponges cf *Pyloderma* sp. and *P. amadou* (**Table 5** and **Figure 7C**). Estimated densities of taxonomic groups are presented in **Supplementary Table 3**.

DISCUSSION

Deep-sea habitats and megafauna biodiversity were described in a limited area across the SPR depth gradient and related to variability of physical factors. Comparable to other ridges in the Atlantic, the slopes of the SPR southern flank were gentle and terraced, mostly covered by biogenic sediments and interrupted by rocky cliffs/crests, dispersed outcrops and loose particles (e.g., the Mid-Atlantic ridge: Priede et al., 2013; Niedzielski et al., 2013; Bell et al., 2016; Alt et al., 2019). Benthic and benthopelagic fauna were generally scarce but spatial variations were noticeable, and potentially driven by depth (and depth covariates), water masses and seascapes zonal distribution. Insufficient sampling precluded attributing causal factors to faunal distribution observed at a meso- and macrohabitat scales. It is possible, however, to assume that observed patterns result from the hierarchical effects of structuring factors operating at different spatial scales (Levin

TABLE 5 | Densities of megafauna (in individuals.m^{-2}) recorded during deep-sea dives in the São Paulo Ridge, SW Atlantic.

Depth Strata	Seascape								
	AMF	**DF**	**BC**	**GF**	**BCR**	**MT**	**GCR**	**Total**	**Area (m^2)**
<2,700 m					**0.3277**	0.0130		**0.1306**	2,014
					0.2996–0.3597	0.0107–0.0157		**0.0504–0.1462**	1,799–2,270
2,700–2,900 m					**0.1309**	**0.1285**	**0.1063**	**0.1091**	2,475
					0.1205–0.1426	**0.1187–0.1388**	**0.0088–0.1140**	**0.1033–0.1152**	2,343–2,615
2,900–3,300 m					0.0736	0.0129	0.0096	0.0226	4,327
					0.0683–0.0797	0.0118–0.0141	0.0088–0.0104	0.0215–0.0238	4,414–4,552
3,300–3,800 m			0.0133		0.0671			0.0204	8,033
			0.0123–0.0144		0.0550–0.0822			0.0189–0.0222	7,390–8,693
>3,800 m	0.0065	0.0040	0.0055	0.0096				0.0052	19,177
	0.0055–0.0075	0.0037–0.0044	0.0050–0.0061	0.0090–0.0100				0.0049–0.0056	17,906–20,590
Total	0.0062	0.0036	0.0099	0.0082	**0.1383**	0.0368	0.0476	0.0257	
	0.0053–0.0073	0.0033–0.0040	0.0093–0.0106	0.0077–0.0088	**0.1291–0.1479**	0.0337–0.0398	0.0449–0.0504	0.0245–0.0268	
Area (m^2)	7,228	4,976	12,394	729	3,087	4,107	2,627		35,609
	6,182–8,560	4,514–5,474	11,603–13,201	683–775	2,887–3,306	3,790–4,482	2,479–1,783		34,075–37,237
AABW (%)	82–94	87–94	20–93	85–92	2–21	0–15	3–9		
NADW (%)	6–18	6–13	7–80	8–15	98–79	85–100	91–97		

Estimated exploration area and densities (means and lower-upper 95%CIs) are presented by seascape unit and depth strata. Numbers in bold highlight the highest densities observed (>0.01 individuals.m^{-2}). Maximum-minimum mixing percentages of the water masses AABW and NADW within the seascape units are expressed in the bottom lines.

et al., 2001; Williams et al., 2010). Allied to bathymetry-derived seafloor morphology segmentation (Brown et al., 2011), reported habitat and megafauna distribution data provided elements to identify scales of spatial variation and to draw hypotheses of potential driving factors.

Biodiversity patterns in the deep SW Atlantic are partly determined by regional (>1,000 km) biogeochemical processes at surface waters. Most of the region down to 30°S lays under the influence the South Atlantic Gyral biogeochemical province (Longhurst, 1995) where surface primary production is generally low due to a stable water column structure and rapid vertical remineralization, resulting in minimal POC export fluxes to the seafloor (Mouw et al., 2016). Schlitzer et al. (2003) estimated POC flux values as low as 0.05–0.1 mol C m^{-2} yr^{-1} in the central South Atlantic, 10–30 times lower than values estimated along the continental margins of West Africa and South America off Brazil. This reduced POC flux reaching the seafloor would tend to support reduced megafauna densities in the SPR (Sibuet et al., 1989; Smith et al., 2008; Wei et al., 2010), as reported in this study (mean 0.026 individuals.m^{-2}; range 0.004–0.350 individuals.m^{-2}). When compared to megafauna densities reported from bathyal areas (2,000–3,500 m) of the North Atlantic (compiled in Levin and Gooday, 2003), densities observed in the SPR (a) approximate values reported in areas under the influence of oligotrophic provinces such as the North Atlantic Subtropical Gyre (0.072 individuals.m^{-2}) and the Caribbean (0.0025 individuals.m^{-2}); and (b) are 2–10 times lower than densities reported in high latitude areas under the influence of eutrophic provinces i.e., the North Atlantic Drift (0.6–0.9 individuals.m^{-2}) and Atlantic Subartic (0.2–1.0 individuals.m^{-2}). Video analysis in bathyal areas of the Mid-Atlantic Ridge northern and southern flanks of the Charlie-Gibbs Fracture Zone (CGFZ, ∼50°N, 2,159–2,601 m depths), revealed megafauna densities varying between 0.92 and 3.4 individuals.m^{-2} and 0.07–0.49 individuals.m^{-2}, respectively, but no relationship with POC flux was established (Bell et al., 2016; Alt et al., 2019). Densities recorded in comparable depths at the SPR (<2,900 m depths; 0.001–0.33 individuals.m^{-2}) were approximately 100 times lower than those recorded to the north of the CGFZ but approximated those recorded to the south.

The regional effect of POC flux on megafauna distribution and abundance is altered by prominent topographic features, such as the SPR and Rio the Grande Rise (RGR), which generate variability in a provincial-scale (∼100–1,000 km). These features disrupt the SW Atlantic basin general morphology (a) producing abrupt discontinuities in depth and slope, (b) modifying the countercurrent flow of the NADW and AABW, and (c) exposing areas of rocky seafloor. The SPR forms a long and linear slope that extends transversely to the South American continental margin north – south orientation and separates a 2,000 m-deep sedimentary plateau (São Paulo), that extends to the north, from a 4,000 m-deep sedimentary-tectonic plateau (Santa Catarina) that extends to the south. This morphology was determined by the tectonic evolution of the South American continental

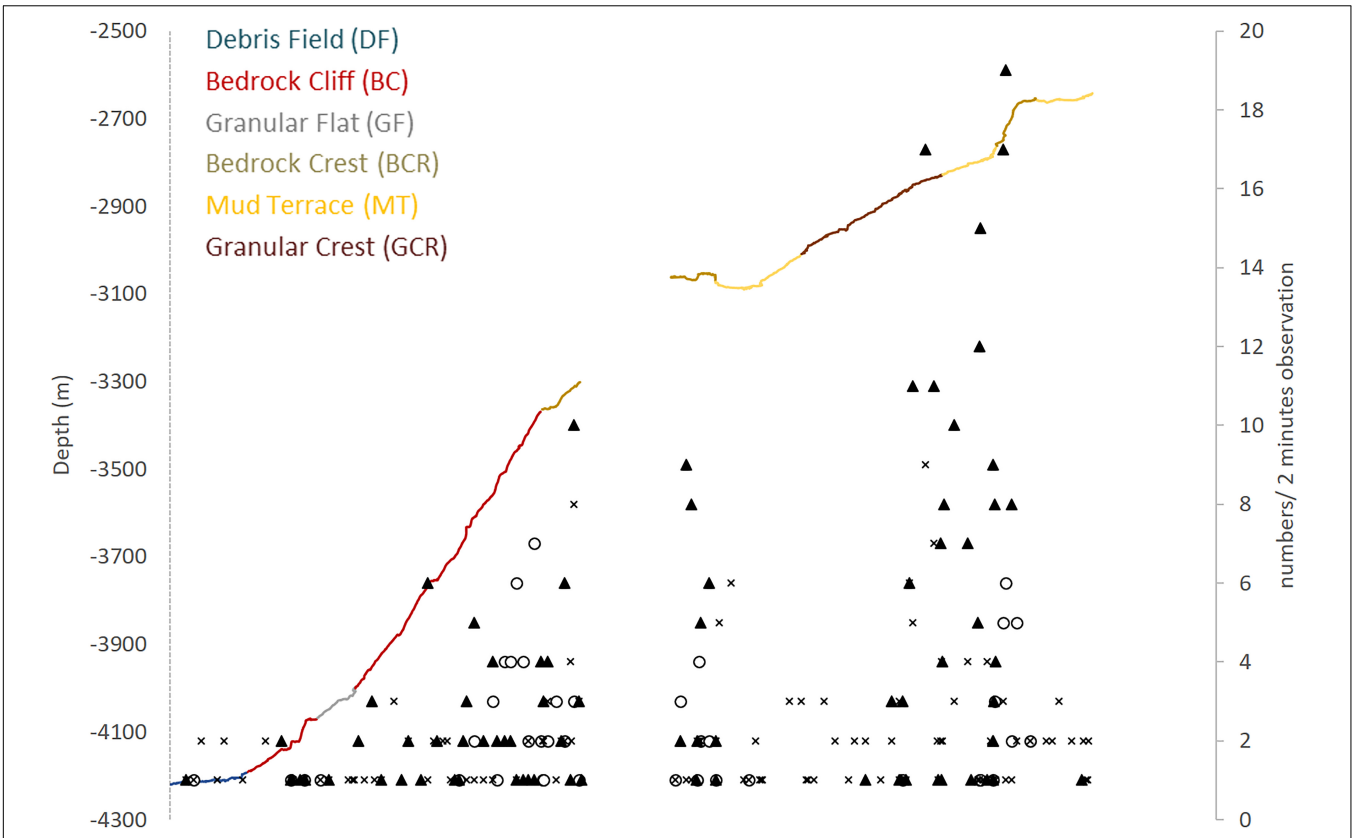

FIGURE 6 | Megafauna distribution along the São Paulo Ridge depth profile explored by deep-sea dives. Abundance of poriferans (dark triangles), anthozoans (empty circles), and other taxa (crosses) is expressed in number of individuals in 2-min observations. Line colors represent different seascape units.

margin and subsequent sedimentary processes, mostly associated with along-slope action of bottom currents and the downslope mass-transport and sediment fluxes (Alberoni et al., 2019). These are processes associated with the flow of NADW and AABW that overlay each other at the slopes of the SPR escarpment (~3,400 m depth), exposing benthic habitats to downslope changes in physical and chemical conditions. In the explored area, temperature increased by nearly 3.0°C (~0.4–3.2 C) over a 1,500 m depth range from the ridge foot (4,200 m) to the ridge crest (2,700 m). Where both water masses mix, at the 3,500–3,300 m depth interval, temperature increased by 1.2°C delimiting lower colder (0.4–1.0°C) and upper warmer (2.0–3.0°C) habitats (**Supplementary Figure 2**). In addition, habitats below this depth interval, under the influence of AABW, also tend to be less oxygenated and less saturated with $CaCO_3$ than those in the upper slope where the influence of NADW predominates (Chung et al., 2003; Rijkenberg et al., 2014). These are contrasting conditions that may partly explain the nearly 10-fold difference in the mean megafauna densities estimated in the SPR depth gradient, below and above 3,400 m depths (**Table 5**). Furthermore, the SPR escarpment interposes the SW Atlantic depth horizons for $CaCO_3$ Aragonite saturation (Ω_{Arg} = 1), Aragonite compensation (ACH), and Calcite saturation (Ω_{Cal} = 1) at ~2,600, ~3,400, and ~4,000 m depths, respectively (Melguen and Thiede, 1974; Thunell, 1982; Chung et al., 2003). These conditions would limit growth of scleractinian cold-water corals in the SPR but not alcyonaceans (Octocorals), which build calcitic skeletons (Roberts et al., 2009). In the explored area such conditions are consistent with the general absence of scleractinian corals and the existing records of bamboo corals (Alcyonacea, Isididae), whose distribution patterns tend to be driven by Calcite saturation levels (Yesson et al., 2012). Finally, topography, depth, temperature, salinity, dissolved O_2 and POC fluxes were all environmental proxies used to define bathyal and abyssal biogeographic provinces (Watling et al., 2013). The SPR is the boundary between a lower bathyal (2,000–3,500 m depths) South Atlantic province and two adjacent abyssal provinces (3,500–6,500 m), the Argentine Basin and the Brazil Basin provinces (Watling et al., 2013). The area explored across the SPR southern flank included the South Atlantic and the Argentine Basin provinces. The drastic changes on megafauna abundance and composition above 3,400 m depths locally support these provinces and the proposed depth boundary.

A variety of megahabitats (~1–100 km) were inferred by seafloor morphology segmentation in the ridge crest, escarpment, plateau and ridge foot zones. Some seafloor structural classes were ground truthed along the depth profile explored by video cameras, despite the different spatial resolution of both methods. In the ridge escarpment, the structural classes "escarp" (Class III.8) and "terrace" (Class III.9) differentiated a lower steeper

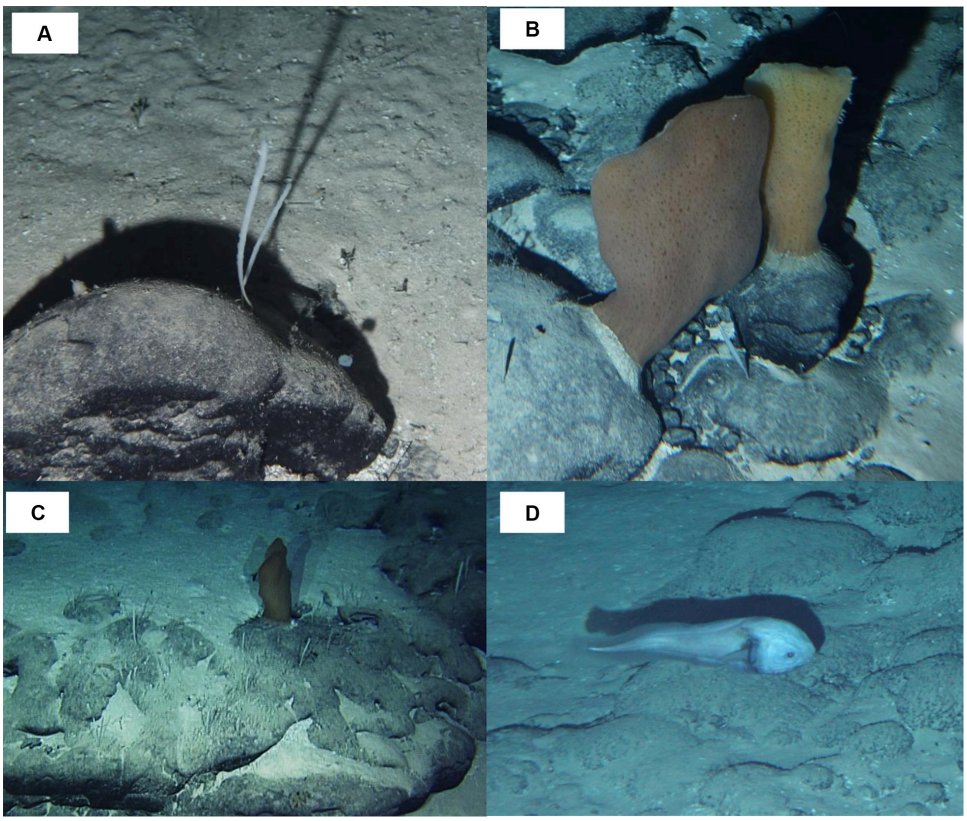

FIGURE 7 | Megafauna observed in São Paulo Ridge, SW Atlantic. **(A)** Dendoricellidae, cf. *Pyloderma* sp. (Demospongiae); **(B,C)** *Poliopogon amadou* (Hexactinellida, Pheronematidae) and *Pyloderma* sp. on rocky outcrops; **(D)** *Acanthonus armatus* (Ophidiiformes, Ophidiidae).

zone from an upper gently sloping zone. This differentiation was evident in the video seafloor analysis, as a steep bedrock cliff changed into a gently sloping bedrock crest seascapes (**Figure 5**), also with a significant increase on the occurrence of sessile suspension feeders (e.g., sponges) and deposit feeders (e.g., holothurians) (**Table 3**). Similar correspondences were also noted at the ridge foot, plateau and ridge crest, suggesting that bathymetry-derived seafloor morphological units were biologically relevant and could express habitat heterogeneity along the SPR. Allied to observations on fauna composition and distribution (see below), biotopes could be predicted and mapped (Brown et al., 2011). However, considerable additional sampling effort would be needed for that purpose (e.g., Robert et al., 2015; Anderson et al., 2016), which was generally beyond the scope of this study (Kitazato et al., 2017).

Nearly half of megafauna records (48%) along the explored depth gradient concentrated in 700–900 m-long patches delimited by the 3,800–3,300 m and 2,900–2,700 m isobaths. The lower zone was covered mostly by rough rocky surfaces whereas the upper zone was characterized by mixed substrates with a predominance of sediments. Despite such differences in substrate composition, megafauna observed in both patches were dominated by sessile suspension feeders (cnidarians and sponges, 73–74% of recorded organisms), followed by benthopelagic organisms (swimming shrimps, fish and cephalopods, 19%) and the less frequent soft bottom dwellers (mostly echinoderms, 6–8%). Suspension feeders did not seem to be limited by hard bottom availability and were commonly recorded even when only a few loose particles (cobbles, pebbles, small outcrops) were available interspersed with dominant sediment substrate. Soft bottom dwellers, on the other hand, were generally scarce despite largely available sedimented areas. Whereas these organisms may be limited by low recruitment rates in the area, records of lebensspuren on the sediment surface could indicate that part of this fauna could be buried in the sediments and not visible in the images. These observations suggest that megafauna spatial distribution at a mesohabitat scale (∼10 s of meters to km) in the explored area of the SPR was (a) less affected by substrate availability, as also reported by studies on the flanks of the Mid-Atlantic Ridge (Bell et al., 2016; Alt et al., 2019), and (b) driven by the availability of suspended food particles, as generated by topography-related current flow patterns over the seafloor.

Both patches of megafauna occurred in the vicinity of crests formed at the edge of terraces (**Figure 6**), where flow dynamics of the NADW may be particularly favorable for sessile suspension feeders (Genin et al., 1986). As a dense water mass flowing over the São Paulo Plateau, the NADW develops a bottom friction transport perpendicular to the depth contour, which, when overlaying a topographic depression such as the SPR escarpment, would drive the NADW flow inside this depression

(Wahlin, 2002). This downslope flow, altered by abrupt changes in slope as observed in the edge of the terraces, could generate areas of vorticity and suspended particle concentrations. In the upper depth zone, evidence of such current action included sand waves observed in sediment cover and movements of the highly dense and flexible sponges *Pyloderma*. Downsloping NADW will encounter AABW opposing flow at 3,400 m depth, within the depth zone of the lower patch of sessile suspension feeders. This water mass interface formed a temperature and salinity gradient as well as a density variation which may characterize a physical boundary condition often associated with POM enrichment (Dullo et al., 2008). Additionally, this density surface (**Supplementary Figure 2**) may also be associated with turbulent mixing (Zhao and Thrunherr, 2017) and along-ridge currents as derived from changes in the AABW transport vorticity as it collides with the SPR southern flank (topographic steering, White and Dorschel, 2010). If these are physical processes occurring to some extent between 3,800 and 3,300 m depths, resuspension or acceleration of advected food particles could favor local settlement and growth of suspension feeders at this depth range. The NADW and AABW interactions extend along the SPR potentially acting at a provincial scale. Yet, because topography is determinant in such physical processes, its effect on megafauna distribution may vary along the ridge, driving variability at smaller spatial scales. In fact, channels and valleys were features modifying the ridge crest, plateau and escarpment overall morphology, potentially altering water flow and sustaining a variety of mesohabitats and patches of suspension feeding fauna.

An Antarctic minke whale skeleton fall was a major driver of megafauna distribution at macrohabitat scale in the debris field seascape (4,204 m depth, Sumida et al., 2016). A series of dispersed vertebrae and intervertebral disks spread over approximately 2 m over the seafloor, comprised over 40 species some of them occurring at high densities in the bone and sediment area (2–70 individuals.m^{-2}). Except from one crustacean (gen. *Munidopsis*), species recorded at and around the whale fall were adapted to organic fall environments and not recorded anywhere else in the SPR explored area.

Most taxa occurrences were recorded from single or very few observations. The exceptions were the sponges *P. amadou* and cf. *Pyloderma* sp., and the benthopelagic fish *A. armatus*, relatively abundant in particular segments of the SPR depth gradient. Despite its uncertain identification, the sponge cf. *Pyloderma* formed the densest epifauna concentrations in the explored area of the SPR. *P. amadou* is the only species of this genus to occur in the Atlantic Ocean, reported in dense patches (up to 5 individuals.m^{-2}) in the Great Meteor seamount (29°30′N; 28°17′W) between 2,675 and 2,765 m depths (Xavier et al., 2015); and in the Tropic Seamount (23°55′N; 20°45′W) where it occurred from 1,960 to 3,660 m depths (Ramiro-Sánchez et al., 2019). In the SPR the species was observed in much lower concentrations (∼0.03–0.06 individuals.m^{-2}) around 3,000 m depth, attached to outcrops and loose rocky particles. *A. armatus* occurs at bathyal and abyssal depths (1,500–4,415 m) in all tropical and subtropical oceans, being particularly abundant in the western Atlantic (Nielsen et al., 1999). The species has been recorded in Brazil's continental margin off Bahia, from 1,171 to 1,929 m (Mincarone et al., 2008) and in the Caribbean between 1,500 and 4,150 m (Polanco et al., 2019). A comparable exploration in the Rio Grande Rise, revealed nearly 3× more fish morphotypes (30) during half the observation time (Perez et al., 2018), potentially because these dives explored much shallower area (1,233–600 m depth). *Bathypterois*, *Spectrunculus*, and *Aldrovandia* were the only genera found in both the SPR and the Rio Grande Rise. In the latter, they were observed only in deepest sectors (1,200–900 m).

The SPR has been characterized as an important area of environmental transitions in the SW Atlantic basin, mostly driven by the depth gradient of its southern flank, where the two main deep-water masses of the Atlantic dynamically interact. Important along-slope chemical and physical gradients are established along the ridge extension, but seafloor morphology, substrate type and topography-driven current flow processes may generate habitat heterogeneity at varying spatial scales, all relevant do deep fauna distribution. Unprecedented observations along the SPR depth profile have generally indicated that megafauna, although scarce, may respond to such drivers and vary considerably in the mesohabitats established along the ridge, justifying future explorations and studies designed to test the effect of the hypothesized drivers (e.g., Bell et al., 2016; Alt et al., 2019).

DATA AVAILABILITY STATEMENT

The raw data supporting the conclusions of this article including videos, sample records and oceanographic data and metadata are available in 'DARWIN – Data and Sample Research System for Whole Cruise Information in JAMSTEC' (http://www.godac.jamstec.go.jp/darwin/).

AUTHOR CONTRIBUTIONS

JP oversaw all aspects of this research, including specimen, sample, data collection, and analysis. All authors conducted the research, analyzed the data, and contributed to the manuscript.

FUNDING

Funding of Brazilian scientists in the "Iata-Piuná" cruise was provided by a grant from CAPES (Program CAPES – JSPS, AUXPE-JSPS-0059–2013, Ministry of Education, Brazil). The senior author was supported by a CPNq productivity fellowship (Process 307992/2019-5). This study was within the umbrella of the National Institute of Science and Technology – Integrated Oceanography Centre (INCT – Mar COI, CNPq).

ACKNOWLEDGMENTS

We thank Brazilian and Japanese governments, and members of JAMSTEC, IOUSP, and CPRM, whose efforts allowed this

unprecedented study in the SW Atlantic, as part of JAMSTEC's "Quelle" expedition. We owe the crews of the RV Yokosuka and the submersible Shinkai 6500 the acquisition of all analyzed data and samples. Eduardo Hajdu, Renato Ventura (Museu Nacional – UFRJ), Thayse Fonseca, and Richard Schwarz (UNIVALI) provided invaluable help with the process of identification of fauna from biological samples and video images. Angelica Maffini Mastella, Carine Eccel, and Anna Caroline Silva de Andrade contributed with video analysis procedures. Katz Fujikura (JAMSTEC) kindly made available high-resolution bathymetry data.

SUPPLEMENTARY MATERIAL

The Supplementary Material for this article can be found online at: https://www.frontiersin.org/articles/10.3389/fmars.2020.572166/full#supplementary-material

REFERENCES

Alberoni, A. A. L., Jeck, I. K., Silva, C. G., and Torres, L. C. (2019). The new Digital Terrain Model (DTM) of the Brazilian Continental Margin: detailed morphology and revised undersea feature names. *Geo-Mar. Lett.* doi: 10.1007/s00367-019-00606-x

Alt, C. H. S., Rogacheva, A. K., Gebruk, A. V., Gooday, A. J., and Jones, D. O. B. (2019). Bathyal benthic megafauna from the Mid-Atlantic Ridge in the region of the Charlie-Gibbs Fracture Zone based on remotely operated vehicle observations. *Deep Sea Res. I* 145, 1–12. doi: 10.1016/j.dsr.2018.12.006

Anderson, O. F., Guinotte, J. M., Rowden, A. A., Clark, M. R., Mormede, S., Davies, A. J., et al. (2016). Field validation of habitat suitability models for vulnerable marine ecosystems in the South Pacific Ocean: Implications for the use of broad-scale models in fisheries management. *Ocean Coast. Manag.* 120, 110–126. doi: 10.1016/j.ocecoaman.2015.11.025

Bassetto, M., Alkimn, F. F., Szatamari, P., and Mohriak, W. U. (2000). "The oceanic segment of the southern Brazilian margin: morpho-structural domains and their tectonic significance," in *Atlantic Rifts and Continental Margins. Geophysical Monograph*, Vol. 115, eds W. Mohriak, and M. Talwani, (Washington, DC: American Geophysical Union), 235–259. doi: 10.1029/gm115p0235

Bell, J. B., Alt, C. H. S., and Jones, D. O. B. (2016). Benthic megafauna on steep slopes at the Northern Mid-Atlantic Ridge. *Mar. Ecol.* 37, 1290–1302. doi: 10.1111/maec.12319

Brown, C. J., Smith, S. J., Lawton, P., and Anderson, J. T. (2011). Benthic habitat mapping: a review of progress towards improved understanding of the spatial ecology of the seafloor using acoustic techniques. *Estuar. Coast. Shelf Sci.* 92, 502–520. doi: 10.1016/j.ecss.2011.02.007

Carney, R. S. (2005). Zonation of deep biota on continental margins. *Oceanogr. Mar. Biol.* 43, 211–278. doi: 10.1201/9781420037449.ch6

Cavalett, A., Silva, M. A. C., Toyofuku, T., Mendes, R., Tekatani, R. G., Pedrini, J., et al. (2017). Dominance of Epsilonproteobacteria associated with a whale fall at a 4204 m depth – South Atlantic Ocean. *Deep Sea Res. II* 146, 53–58. doi: 10.1016/j.dsr2.2017.10.012

Chung, S. N., Lee, K., Feely, R. A., Sabine, C. L., Millero, F. J., Wanninkhof, R., et al. (2003). Calcium carbonate budget in the Atlantic Ocean based on water column inorganic carbon chemistry. *Glob. Biogeochem. Cycles* 17: 1093.

Dullo, W., Flogell, S., and Ruggerberg, A. (2008). Cold-water coral growth in relation to the hydrography of the Celtic and Nordic European continental margin. *Mar. Ecol. Prog. Ser.* 371, 165–176. doi: 10.3354/meps07623

Erdey-Heydorn, M. D. (2008). An ArcGIS seabed characterization toolbox developed for investigating benthic habitats. *Mar. Geod.* 31, 318–358. doi: 10.1080/01490410802466819

Frajka-Williams, E., Ansorje, I. J., Baerh, J., Bryden, H. L., Chidichimo, M. P., Cunninhan, S. A., et al. (2019). Atlantic meridional overturning circulation: observed transport and variability. *Front. Mar. Sci.* 6:260. doi: 10.3389/fmars.2019.00260

Gamboa, L. A. P., and Kumar, N. (1977). Synthesis of geological and geophysical data in a 1° square area around site 356, leg 39 DSDP. *Deep Sea Drilling Project* 39, 947–954. doi: 10.2973/dsdp.proc.39.141.1977

Gamboa, L. A. P., and Rabinowitz, P. D. (1981). The Rio Grande Fracture Zone in the Western South Atlantic and its tectonic implications. *Earth Planet. Sci. Lett.* 52, 410–418. doi: 10.1016/0012-821x(81)90193-x

Garzoli, S. L., and Matano, R. P. (2011). The South Atlantic and the Atlantic meridional overturning circulation. *Deep Sea Res. II* 58, 1837–1847. doi: 10.1016/j.dsr2.2010.10.063

Genin, A., Dayton, P. K., Lonsdale, P. F., and Spiess, F. N. (1986). Corals on seamount peaks provide evidence of current acceleration over deep-sea topography. *Nature* 322, 59–61. doi: 10.1038/322059a0

Greene, H. G., Bizzarro, J. J., O'Connell, V. M., and Brylinsky, C. K. (2007). Construction of digital potential marine benthic habitat maps using a code classification scheme and its application. *Geol. Associat Canada Spec. Pap.* 47, 141–155.

Greene, H. G., Yoklavich, M. M., Starr, R. M., O'Connell, V. M., Wakefield, W. W., Sullivan, D. E., et al. (1999). A classification scheme for deep seafloor habitats. *Oceanol. Acta* 22, 663–678. doi: 10.1016/s0399-1784(00)88957-4

Hajdu, E., Castello-Branco, C., Lopes, D. A., Sumida, P. Y. G., and Perez, J. A. A. (2017). Deep-sea dives reveal an unexpected hexactinellid sponge garden on the Rio Grande Rise (SW Atlantic). A mimicking habitat? *Deep-Sea Res. II* 146, 93–100. doi: 10.1016/j.dsr2.2017.11.009

Hein, J. R., Mizell, K., Koschinski, A., and Conrad, T. A. (2013). Deep-ocean mineral deposits as a source of critical metals for high- and green-technology applications: comparison with land-based resources. *Ore Geol. Rev.* 51, 1–14. doi: 10.1016/j.oregeorev.2012.12.001

Ichisima, H., Augustin, A. H., Toyofuku, T., and Kitazato, H. (2017). A new species of Africanacetus (Odontoceti: Ziphiidae) found on the deep ocean floor off the coast of Brazil. *Deep Sea Res. II* 146, 68–81. doi: 10.1016/j.dsr2.2016.12.002

Jones, D. O. B., Bett, B. J., Wynn, R. B., and Masson, D. G. (2009). The use of towed camera platforms in deep-water science. *Underw. Technol.* 28, 41–50. doi: 10.3723/ut.28.041

Jovane, L., Hein, J. R., Yeo, I. A., Benites, M., Bergo, N. M., Corrêa, P. V., et al. (2019). Multidisciplinary scientific cruise to the Rio Grande Rise. *Front. Mar. Sci.* 6:252. doi: 10.3389/fmars.2019.00252

Kitazato, H., Fujikura, K., Pellizari, V., Perez, J. A. A., and Sumida, P. (2017). Editorial: Rich geo- and bio-diversities exist in the South West Atlantic deep-sea: the first human-occupied submersible Shinkai 6500 dive cruise (Iatá-piúna). *Deep Sea Res. II* 146, 1–3. doi: 10.1016/j.dsr2.2017.11.007

Levin, L., and Gooday, A. J. (2003). "The Deep Atlantic Ocean," in *Ecosystems of the Deep Oceans. Ecosystems of the World*, Vol. 28, ed. P. A. Tyler, (Amsterdam: Elsevier), 111–178.

Levin, L. A., Etter, R. J., Rex, M. A., Gooday, A. J., Smith, C. R., Pineda, J., et al. (2001). Environmental influences on regional deep-sea species diversity. *Annu. Rev. Ecol. Syst.* 32, 51–93. doi: 10.1146/annurev.ecolsys.32.081501.114002

Longhurst, A. (1995). Seasonal cycles of pelagic production and consumption. *Prog. Oceanog.* 36, 77–176. doi: 10.1016/0079-6611(95)00015-1

Mamayev, O. I. (1975). *Temperature-Salinity Analysis of World Ocean Waters*, Vol. 11. Amsterdam: Elsevier Science,.

McDonagh, E. L., Arhan, M., and Heywood, K. J. (2002). On the circulation of bottom water in the region of the Vema Channel. *Deep Sea Res. I* 49, 1119–1139. doi: 10.1016/s0967-0637(02)00016-x

Melguen, M., and Thiede, J. (1974). Facies distribution and dissolution depths of surface sediment components from the Vema channel and the Rio Grande rise (southwest Atlantic Ocean). *Mar. Geol.* 17, 341–353. doi: 10.1016/0025-3227(74)90096-6

Mincarone, M. M., Nielsen, J. G., and Costa, P. A. S. (2008). Deep-sea ophidiiform fishes collected on the Brazilian continental slope, between 11° and 23°S. *Zootaxa* 1770, 41–64. doi: 10.11646/zootaxa.1770.1.2

Montserrat, F., Guilhon, M., Corrêa, P. V. F., Bergo, N. M., Signori, C. N., Turra, P. M., et al. (2019). Deep-sea mining on the Rio Grande Rise (Southwestern Atlantic): a review on environmental baseline. Ecosystem services and potential impacts. *Deep Sea Res. I* 145, 31–58. doi: 10.1016/j.dsr.2018.12.007

Morozov, E., Demidov, A., Tarakanov, R., and Zenk, W. (2010). *Abyssal Channels in the Atlantic Ocean: Water Structure and Flows*. Dordrecht: Springer.

Mouw, C. B., Barnett, A., McKinley, G. A., Gloege, L., and Pilcher, D. (2016). Phytoplankton size impact on export flux in the global ocean. *Glob. Biogeochem. Cycles* 30, 1542–1562. doi: 10.1002/2015GB005355

Nakajima, R., Komuku, T., Yamakita, T., Lindsay, D. J., Jintsu-Uchifune, Y., Watanabe, H., et al. (2014). A new method for estimating the area of the seafloor from oblique image taken by deep-sea submersible survey platforms. *JAMSTEC Rep. Res. Dev.* 19, 59–66. doi: 10.5918/jamstecr.19.59

Niedzielski, T., Høines, A., Shields, M. A., Linley, T. D., and Priede, I. G. (2013). A multi-scale investigation into seafloor topography of the northern Mid-Atlantic Ridge based on geographic information system analysis. *Deep Sea Res. II* 98, 231–243. doi: 10.1016/j.dsr2.2013.10.006

Nielsen, J. G., Cohen, D. M., Markle, D. F., and Robins, C. R. (1999). "Ophidiiform fishes of the world (Order Ophidiiformes)," *An annotated and Illustrated Catalogue of Pearlfishes, Cusk-eels, Brotulas and other Ophidiiform Fishes Known to Date.* FAO Fisheries Synopsis. No. 125, Vol. 18, (Rome: FAO).

Perez, J. A. A., Alves, E. S., Malcolm, C., Bergstad, O. A., Gebruk, A., Cardoso, I. A., et al. (2012). Patterns of life on the southern mid-atlantic ridge: compiling what is known and addressing future research. *Oceanography* 25, 16–31. doi: 10.5670/oceanog.2012.102

Perez, J. A. A., Kitazato, H., Sumida, P. Y. G., Sant'Ana, R., and Mastella, A. M. (2018). Benthopelagic megafauna assemblages of the Rio Grande Rise (SW Atlantic). *Deep Sea Res. I* 134, 1–11. doi: 10.1016/j.dsr.2018.03.001

Polanco, A., Dueñas, L. F., Leon, J., and Puentes, V. (2019). New records and update on the geographic distribution of the Bonyeared Assfish, Acanthonus armatus Günther, 1878 (Ophidiidae, Neobythitinae), in the Caribbean region. *Check List.* 15, 767–772. doi: 10.15560/15.5.767

Priede, E. G., Bergstad, O. A., Miller, P. I., Vecchione, M., Gebruk, A., Falkenhaug, T., et al. (2013). Does presence of a mid-ocean ridge enhance biomass and biodiversity? *PLoS One* 8:e61550. doi: 10.1371/journal.pone.0061550

Ramiro-Sánchez, B., González-Irusta, J. M., Henry, L., Cleland, J., Yeo, I., Xavier, J. R., et al. (2019). Characterization and mapping of a deep-sea sponge ground on the tropic seamount (Northeast Tropical Atlantic): implications for spatial management in the high seas. *Front. Mar. Sci.* 6:278. doi: 10.3389/fmars.2019.00278

Rex, M. A., and Etter, R. J. (2010). *Deep-Sea Biodiversity. Pattern and Scale*. Cambridge, MA: Harvard University Press.

Rijkenberg, M. J. A., Middag, R., Laan, P., Gerringa, L. J. A., Van Aken, H. M., et al. (2014). The distribution of dissolved iron in the West Atlantic Ocean. *PLoS One* 9:e101323. doi: 10.1371/journal.pone.0101323

Robert, K., Jones, D. O. B., Tyler, P. A., Van Rooij, D., and Huvenne, V. A. I. (2015). Finding the hotspots within a biodiversity hotspot: fine-scale biological predictions within a submarine canyon using high-resolution acoustic mapping techniques. *Mar. Ecol.* 36, 1256–1276. doi: 10.1111/maec.12228

Roberts, J. M., Wheeler, A. J., Freiwald, A., and Cairns, S. D. (2009). *The Biology and Geology of Deep-Sea Coral Habitats*. Cambridge: Cambridge University Press.

Schlitzer, R., Usbeck, R., and Fischer, G. (2003). "Inverse modelling of particulate organic carbon fluxes in the South Atlantic," in *The South Atlantic in the Late Quaternary: Reconstruction of Material Budgets and Current Systems*, eds G. Wefer, S. Mulitza, and V. Ratmeyer, (Berlin: Springer-Verlag), 1–19. doi: 10.1007/978-3-642-18917-3_1

Shimabukuro, M., Rizzo, A. E., Alfaro-Lucas, J. M., Fujiwara, Y., and Sumida, P. Y. G. (2017). *Sphaerodoropsis kitazatoi*, a new species and the first record of Sphaerodoridae (Annelida: Phyllodocida) in SW Atlantic abyssal sediments around a whale carcass. *Deep Sea Res. II* 146, 18–26. doi: 10.1016/j.dsr2.2017.04.003

Shimabukuro, M., and Sumida, P. Y. G. (2019). Diversity of bone-eating Osedax worms on the deep Atlantic whale falls—bathymetric variation and inter-basin distributions. *Mar. Biodiver.* 49, 2587–2599. doi: 10.1007/s12526-019-00988-2

Sibuet, M., Lambert, C. E., Chesselet, R., and Laubier, L. (1989). Density of the major size groups of benthic fauna and trophic input in deep basins of the Atlantic Ocean. *J. Mar. Res.* 47, 851–867. doi: 10.1357/002224089785076064

Smith, C. R., De Leo, F. C., Bernardino, A. F., Sweetman, A. K., and Arbizu, P. M. (2008). Abyssal food limitation, ecosystem structure and climate change. *Trends Ecol. Evolut.* 23, 518–528. doi: 10.1016/j.tree.2008.05.002

Stramma, L., and England, M. (1999). On the water masses and mean circulation of the South Atlantic Ocean. *J. Geophys. Res.* 104, 20863–20883. doi: 10.1029/1999jc900139

Sumida, P. Y. G., Alfaro-Lucas, J. M., Shimabukuro, M., Kitazato, H., Perez, J. A. A., Soares-Gomes, A., et al. (2016). Deep-sea whale fall fauna from the Atlantic resembles that of the Pacific Ocean. *Sci. Rep.* 6:22139. doi: 10.1038/srep22139

Thunell, R. C. (1982). Carbonate dissolution and abyssal hydrography in the Atlantic Ocean. *Mar. Geol.* 47, 165–180. doi: 10.1016/0025-3227(82)90067-6

Tissot, B. (2008). "Video analysis, experimental design, and database management of submersible-based habitat studies," in *Marine Habitat Mapping Technology for Alaska*, eds J. R. Reynolds, and H. G. Greene, (Fairbanks, AK: Alaska University of Alaska Fairbanks), doi: 10.4027/mhmta.2008.11

Tissot, B. N., Hixon, M. A., and Stein, D. L. (2007). Habitat-based submersible assessment of macro-invertebrate and groundfish assemblages at Heceta Bank, Oregon, from 1988 to 1990. *J. Exp. Mar. Biol. Ecol.* 352, 50–64. doi: 10.1016/j.jembe.2007.06.032

Ussami, N., Chaves, C. A. M., Marques, L. S., and Ernesto, M. (2012). "Origin of Rio Grande Rise – Walvis Ridge reviewed integrating palaeogeographic reconstruction, isotope geochemistry and flexural modelling," in *Conjugate Divergent Margins*, eds W. U. Mohriak, A. Danforth, P. J. Post, D. E. Brown, G. C. Tari, M. Nemcok, et al. (London: Geological Society London, Special Publication), 369.

Wahlin, A. K. (2002). Topographic steering of dense currents with application to submarine canyons. *Deep Sea Res. I* 49, 305–320. doi: 10.1016/s0967-0637(01)00058-9

Walbridge, S., Slocum, N., Pobuda, M., and Wright, D. J. (2018). Unified geomorphological analysis workflows with benthic terrain modeler. *Geosciences* 8:94. doi: 10.3390/geosciences8030094

Watling, L., Guinotte, J. M., Clark, M., and Smith, C. (2013). A proposed biogeography of the deep ocean floor. *Progr. Oceanogr.* 111, 91–112. doi: 10.1016/j.pocean.2012.11.003

Wei, C., Rowe, G. T., Escobar-Briones, E., Boetius, A., Soltwedel, T., Caley, M. J., et al. (2010). Global patterns and predictions of seafloor biomass using random forests. *PLoS One* 5:e15323. doi: 10.1371/journal.pone.0015323

White, M., and Dorschel, B. (2010). The importance of the permanent thermocline to the cold water coral carbonate mound distribution in the NE Atlantic. *Earth Planet. Sci. Lett.* 296, 395–402. doi: 10.1016/j.epsl.2010.05.025

Williams, A., Althaus, F., Dunstan, P. K., Poore, G. C. B., Bax, N. J., Kloser, R. J., et al. (2010). Scales of habitat heterogeneity and megabenthos biodiversity on an extensive Australian continental margin (100–1100 m depths). *Mar. Ecol.* 31, 222–236. doi: 10.1111/j.1439-0485.2009.00355.x

Wilson, M. F. J., O'Connel, B., Brown, C., Guinan, J. C., and Grehan, A. J. (2007). Multiscale terrain analysis of multibeam bathymetry data for habitat mapping on the continental slope. *Mar. Geod.* 30, 3–35. doi: 10.1080/01490410701295962

Xavier, J. R., Tojeira, I., and van Soest, E. W. M. (2015). On a hexactinellid sponge aggregation at the Great Meteor seamount (North-east Atlantic). *J. Mar. Biol. Assoc. U.K.* 95, 1389–1394. doi: 10.1017/S0025315415000685

Yesson, C., Taylor, M. L., Tittensor, D. P., Davies, A. J., Guinotte, J., Baco, A., et al. (2012). Global habitat suitability of cold-water octocorals. *J. Biogeogr.* 39, 1278–1292. doi: 10.1111/j.1365-2699.2011.02681.x

Zhao, J., and Thrunherr, A. M. (2017). Changes in bottom water physical properties above the MAR flank in the Brazil Basin. *JGR Oceans* 123, 708–719. doi: 10.1002/2017jc013375

Conflict of Interest: The authors declare that the research was conducted in the absence of any commercial or financial relationships that could be construed as a potential conflict of interest.